PHYSICAL SCIENCES

COMPARATIVE STUDY OF THE MOLECULAR DYNAMICS OF ANTHRACENE AND ONE OF ITS DERIVATIVE (1-HYDROXYANTHRACENE)IN GAS PHASE AND ETHANOL: RHF AND DFT STUDY

[1]Umar, G., Chifu E. [2]Ndikilar and [1]John S. M.
[1]Physics Department, Nasarawa State University, Keffi, Nigeria
[2]Physics Department, Federal University Dutse, P.M.B 7156, Dutse, Jigawa State, Nigeria
Corresponding email: adaturu21@gmail.com

Manuscript received 20/02/2016 Accepted: 30/12/2016 Published: December, 2016

ABSTRACT

A comparative study of the molecular geometries of the organic semi-conductor material Anthracene and one of its derivative (1-hydroxyanthracene) in gas phase and ethanol is studied at the Restricted-HartreeFock (RHF) and Density Functional Theory (DFT) levels of theory by employing 6-31G basis set. The molecular structure, dipole moment, quadrupole moment, charge transfer, polarizability, energy and vibrational frequencies with Infrared (IR) and Raman intensities have been studied. Frequency analysis was carried out in all the cases to ensure that the optimized geometries correspond to total energy minima. At both level of theory it is predicted that the solvent (ethanol) has an effect of expanding the molecules as there is slight increase in most of the bond lengths, bond angles and dihedral angles as compare to gas phase analysis. For anthracene it is predicted that the bonds with the lowest bond lengths are R(1,17), R(6,20), R(13,22), R(14,23) with a bond length of 1.0719 Å in gas phase and ranging from 1.0751 to 1.0771 Armstrong in ethanol at the RHF level of theory while for 1 Hydroxyanthraceneit is predicted that the bond with the lowest bond length is R(7,15) with a bond length of 1.0712 Å in gas phase and 1.0733 Å in ethanol at the RHF level of theory. The predicted dipole moment for Anthracene is almost zero at RHF/6-31G level and zero at B3LYP/6-31G level indicating that the molecule is not polar and the charge distribution is fairly symmetrical. The magnitude of the dipole moment obtained at B3LYP/6-31G level is slightly higher as compared to the corresponding values of the dipole moment at RHF/6-31G level. The quadrupole moment predicts that all two molecules are slightly elongated along the ZZ axis, with 1 Hydroxyanthracene showing the highest elongation at both levels of theory.

INTRODUCTION

The properties of Anthracene derivative 1-hydroxyanthracene in their anionic, neutral and cationic charge states have been investigated using the density functional theory (Kukhta *et al*., 2011). The effect of addition and removal of the electron on the bond lengths, atomic charges, and frontier orbitals, ionization potential (IP), electron affinity (EA) and reorganization energy was considered in their study. Detailed polarized absorption and emission spectra for anthracene and some of its methyl and methoxy derivatives in rigid solution at 77°K have been studied (Friedrich *et al.,* 2004). PPP-SCF calculations show that no new states are introduced below 5 eV by the substitution. The observed effects of chemical substitution on state ordering, polarizations and oscillator strength correlate quite well with the predictions of the PPP-SCF calculations. A vibrational analysis of the anthracene polarization spectra is carried out. In the near long-axis polarized absorption and fluorescence of anthracene, two vibronic origins are identified as a 1630 $cm^{-1}b_1g$ molecular vibration and a weak 60 $cm^{-1}bg$ type of lattice vibration. All long-axis polarized structure in the near absorption can be assigned to Franck-Condon progressions built upon these vibronic origins in the ^1La band (which is electronically short-axis polarized). Differences in the spectral integrated transition intensity (oscillator strength) between the absorption and the emission reveal an additional long-axis component in the high energy region of the ^1La absorption which could be evidence for the hidden ^1Lb band in anthracene. However, there is no clear cut structural evidence for this state in the polarization spectrum. This hidden transition is allowed by methoxy substitution. In the symmetric 2,3-dimethoxyanthracene, the ^1Lb band appears at 365 nm as a new transition. In 2-methoxyanthracene the ^1La and the ^1Lb are strongly mixed. The anomalous *short-axis* polarization of the ^1Lb band, predicted by the theory for 2-methoxyanthracene, is confirmed by the polarization data. Methoxy substitution also reveals new weak bands, located between the ^1Lb and ^1Bb bands, of B_1g and A_1g parentage, which are successfully predicted by the PPP-SCF calculations. Naoto and Atsushi(2007), investigated the evolution of the electronic structure of molecular aggregates using anion photoelectron (PE) spectroscopy for anionic clusters of anthracene (Ac) and its alkyl derivatives: 1-methylanthracene (1MA), 2-methylanthracene (2MA), 9-methylanthracene (9MA), 9,10-dimethylanthracene (DMA), and 2-*tert*-butylanthracene (2TBA). For their monomer anions (n = 1), electron affinities are confined to the range from 0.47 to 0.59 eV and are well reproduced by density functional theory calculations, showing the isoelectronic character of these molecules. For cluster anions (n = 2–100) of Ac and 2MA, two types of isomers I and II coexist over a wide size range: isomers I and II-1 (n<30) or isomers I and II-2 (n ≥ ~40 for Ac and n ≥~55 for 2MA). However, for the other alkyl-substituted Ac cluster anions (i.e., 1MA, 9MA, DMA, and 2TBA), only isomer I is exclusively formed, and neither isomer II-1 nor II-2 is observed. It highlights some of the molecular dynamic properties that are essential for the development of future opto-electronic devices. Organic semi-conductors have many advantages, such as, easy fabrication, mechanical flexibility and low cost (James, 2007).

MATERIALS AND METHODS

The Schrodinger equation for a collection of particles like a molecule is very similar to that of a particle. In this case, Ψ, the wave function would be a function of the coordinates of all the particles in the system as well as the time, t. The energy and many other properties of the particle can be obtained by solving the Schrodinger equation for , subject to the appropriate boundary conditions. Many different wave functions are solutions to it, corresponding to different stationary states of the system.

For a molecular system, Ψ is a function of the positions of the electrons and the nuclei within the molecule, which we will designate as $\vec{r}$ and $\vec{R}$, respectively. These symbols are shorthand for the set of component vectors describing the position of each particle. Note that electrons are treated individually, while each nucleus is treated as an aggregate; the component nucleons are not treated individually.

The kinetic energy is a summation of ∇^2 over all the particles in the molecule:

$$T=-\frac{h^2}{8\pi^2}\sum_k \frac{1}{m_k}\left(\frac{\partial^2}{\partial x_k^{\,2}}+\frac{\partial^2}{\partial y_k^{\,2}}+\frac{\partial^2}{\partial z_k^{\,2}}\right) \quad \text{.....(2.1)}$$

The potential energy component is the Coulomb repulsion between each pair of charged entities (treating each atomic nucleus as a single charged mass):

$$V=\frac{1}{4\pi\varepsilon_0}\sum_j \sum_{k<j}\frac{e_j e_k}{\Delta r_{jk}} \quad \text{.....(2.2)}$$

Where is the distance between the two particles, and and are the charges on particles j and k. For an electron the charge is –e, while for a nucleus, the charge is Ze, where Z is the atomic number for that atom. Thus,

$$V=\frac{1}{4\pi\varepsilon_0}\left\{-\sum_i\sum_I\frac{Z_I e^2}{\Delta r_{iI}}+\sum_i\sum_{j<i}\frac{e^2}{\Delta r_{ij}}+\sum_I\sum_{J<I}\frac{Z_I Z_J e^2}{\Delta R_{IJ}}\right\} \quad \text{.....(2.3)}$$

The first term corresponds to electron-nuclear attraction, the second to electron-electron repulsion and the third to nuclear-nuclear repulsion (Lee *et al*., 1988).

The Born-Oppenheimer approximation is the first of several approximations used to simplify the solution of the Schrodinger equation. It simplifies the general molecular problem by separating nuclear and electronic motions. This approximation is reasonable since the mass of a typical nucleus is thousands of times greater than that of an electron. The full Hamiltonian for the molecular system can then be written as:

$$H=T^{elec}(\vec{r})+T^{nucl}(\vec{R})+V^{nucl-elec}(\vec{R},\vec{r})+V^{elec}(\vec{r})+V^{nucl}(\vec{R}) \quad \text{.....(2.4)}$$

The Born-Oppenheimer approximation allows the two parts of the problem to be solved independently, so we can construct an electron Hamiltonian which neglects the kinetic energy term for the nuclei. This Hamiltonian is then used in the Schrodinger equation describing the motion of electrons in the field of fixed nuclei.

ψ^2 is interpreted as the probability density for the particle(s) it describes. Therefore, we require that ψ be normalized; if we integrate over all space, the probability should be the number of particles. Accordingly, we multiply ψ by a constant such that:

$$\int_{-\infty}^{+\infty}|c\psi|^2\,dv=n_{particles} \quad \text{.....(2.5)}$$

We can do this because the Schrodinger equation is an eigenvalue equation, and in general, if f is a solution to an eigenvalue equation, then cf is also, for any value of $\boldsymbol{c}$ (Coates, J., 2000). The first approximation to be considered comes from the interpretation of $|\psi|^2$ as a probability density for the electrons within the system. Molecular orbital theory decomposes ψ into a combination of molecular orbitals: ϕ_1 , ϕ_2 , …. To fulfill some of the conditions on ψ , a normalized, orthogonal set of molecular orbitals is chosen as:

$$\iiint\phi_i^*\phi_i\,dxdydz=1$$

$$\iiint\phi_i^*\phi_j\,dxdydz=0 \qquad i\neq j \quad \text{.....(2.6)}$$

The simplest possible way of making ψ as a combination of these molecular orbitals is by forming their Hartree product (Friedrich *et al*., 2004).

$$\psi(\vec{r})=\phi_1(\vec{r}_1)\phi_2(\vec{r}_2)...\phi_n(\vec{r}_n) \quad \text{.....(2.7)}$$

The simplest anti-symmetric function that is a combination of molecular orbitals is a determinant. However, most calculations are closed shell calculations, using doubly occupied orbitals, holding two electrons of opposite spin. For the moment, we will limit our discussion to this case.

We define two spin functions, α and β as follows:

$$\alpha(\uparrow)=1 \qquad \alpha(\downarrow)=0$$

$$\beta(\uparrow)=0 \qquad \beta(\downarrow)=1 \quad \text{.....(2.8)}$$

The α function is 1 for a spin up electron and the β function is 1 when the electron is spin down. The notation $\alpha(i)$ and $\beta(i)$ will designate the values of α and β for electron i ; thus $\alpha(1)$ is the value of α for electron 1. We can now build a closed shell wave function by defining $n/2$ molecular orbitals for a system with n electrons and then assigning electrons to these orbitals in pairs of opposite spin.

$$\psi(\vec{r})=\frac{1}{\sqrt{n!}}\begin{vmatrix}\phi_1(\vec{r}_1)\alpha(1) & \phi_1(\vec{r}_1)\beta(1) & \phi_2(\vec{r}_1)\alpha(1) & \phi_2(\vec{r}_1)\beta(1)...\phi_{n/2}(\vec{r}_1)\alpha(1) & \phi_{n/2}(\vec{r}_1)\beta(1)\\ \phi_1(\vec{r}_2)\alpha(2) & \phi_1(\vec{r}_2)\beta(2) & \phi_2(\vec{r}_2)\alpha(2) & \phi_2(\vec{r}_2)\beta(2)...\phi_{n/2}(\vec{r}_2)\alpha(2) & \phi_{n/2}(\vec{r}_2)\beta(2)\\ \cdots & \cdots & \cdots & \cdots & \cdots\\ \phi_1(\vec{r}_n)\alpha(n) & \phi_1(\vec{r}_n)\beta(n) & \phi_2(\vec{r}_n)\alpha(n) & \phi_2(\vec{r}_n)\beta(n)...\phi_{n/2}(\vec{r}_n)\alpha(n) & \phi_{n/2}(\vec{r}_n)\beta(n)\end{vmatrix} \quad \text{...(2.9)}$$

Each row is formed by representing all possible assignments of electron i to all orbital-spin combinations. The initial factor is necessary for normalization. Swapping two electrons corresponds to interchanging two rows of the determinant, which will have the effect of changing its sign.

The next approximation involves expressing the molecular orbitals as linear combinations of a pre-defined set of one-electron function known as basis functions. These functions are usually centered on the atomic nuclei and so bear some resemblance to atomic orbitals. However, the actual mathematical treatment is more general than this and any set of appropriately defined functions may be used Naoto and Atsushi (2007).An individual molecular orbital is defined as:

$$\phi_i=\sum_{\mu=1}^{N}c_{\mu i}\chi_\mu \quad \text{.....(2.10)}$$

where the coefficients $c_{\mu i}$ are known as the molecular orbital expansion coefficients. The basis functions $\chi_1....\chi_N$ are also chosen to be normalized. Gaussian and other ab initio electronic structure programs use gaussian-type atomic functions as basis functions. Gaussian functions have the general form:

$$g(\alpha,\vec{r})=cx^n y^m z^l e^{-\alpha r^2} \quad \text{.....(2.11)}$$

Where is composed of x, y and z. α is a constant determining the size (radial extent) of the function.

In a gaussian function, $e^{-\alpha r^2}$ is multiplied by powers of x, y and z, and a constant for normalization, so that:

$$\int_{all\ space} g^2 = 1 \quad \text{.....(2.12)}$$

Thus, c depends on α , *l, m* and *n*.Here are three representative gaussian functions (s, p_y and d_{xy} types, respectively):

$$g_s(\alpha, \vec{r}) = \left(\frac{2\alpha}{\pi}\right)^{3/4} e^{-\alpha r^2}$$

$$g_y(\alpha, \vec{r}) = \left(\frac{128\alpha^5}{\pi^3}\right)^{1/4} ye^{-\alpha r^2} \quad \text{.....(2.13)}$$

$$g_{xy}(\alpha, \vec{r}) = \left(\frac{2048\alpha^7}{\pi^3}\right)^{1/4} xye^{-\alpha r^2}$$

Linear combinations of primitive gaussians like these are used to form the actual basis functions; the latter are called contracted gaussians and have the form:

$$\chi_\mu = \sum_p d_{\mu p} g_p \quad \text{.....(2.14)}$$

Where the $d_{\mu p}$'s are fixed constants within a given basis set. Note that contracted functions are also normalised in common practice.

All of these constructions result in the following expansion for molecular orbitals:

$$\phi_i = \sum_\mu c_{\mu i}\chi_\mu = \sum_\mu c_{\mu i}\left(\sum_p d_{\mu p} g_p\right) \quad \text{.....(2.15)}$$

The problem has now become how to solve for the set of molecular orbital expansion coefficients, $c_{\mu i}$

Hartree-Fock theory takes advantage of the variational principle, which says that for the ground state of any antisymmetric normalized function of the electronic coordinates, which we will denote Ξ , then the expectation value for the energy corresponding to Ξ will always be greater than the energy for the exact wavefunction:

$$E(\Xi) > E(\Psi) \qquad \Xi \neq \Psi \quad \text{.....(2.16)}$$

RESULTS AND DISCUSSION

Geometry optimizations usually attempt to locate minima on the potential energy surface, thereby predicting equilibrium structures of molecular systems (Frisch, 2004). At the minima, the first derivative of the energy (gradient) is zero. Since the gradient is the negative of the forces, the forces are also zero at such a point (stationary point). In Gaussian, a geometry optimization begins at the molecular structure specified at the input and steps along the potential energy surface. It computes the energy and gradient at that point, and determines which direction to make the next step. The gradient indicates the direction along the surface in which the energy decreases most rapidly from the current point as well as the steepness of that slope. The optimized parameters are the bond lengths (in Armstrong), the bond angles and the dihedral angles for the optimized molecular structure. Atoms in the molecule are numbered according to their order in the molecule specification section of the input(Umar and Chifu, 2012).

Optimized Molecular Parameters of Anthracene and 1-hydroxyanthracene

The optimized bond lengths of Anthracene in gas phase and ethanol are listed in Table 1. The optimized molecular structure is shown in Figure 1. The predicted bond lengths in gas phase at RHF/6-31G level are slightly smaller than the corresponding values in solution (ethanol) and the same is obtained at the DFT/B3LYP/6-31G level of theory. Changes in bond lengths are noticed when one goes from the RHF/6-31G to B3LYP/6-31G level, but no significant change in the bond angles is noticed in the gas phase. It seems inclusion of electron correlation expands the molecule. It is predicted that the bonds with the least bond lengths are R(1,17), R(6,20), R(13,22) and R(14,23) with a bond length of 1.0719 Å in gas at RHF level of theory. These are all C-H bonds. Thus it is predicted that the strongest bonds in Anthracene molecule are the C-H bonds. The bonds with the longest bond lengths in gas phase at RHF level of theory are R(2,3), R(4,5), R(9,15) and R(10,11) with a bond length of 1.4341 Å in gas phase at RHF level of theory which are all C=C bonds. This indicates that the C=C bonds are the weakest. Since solvation in ethanol increases the bond length at both levels of theory, it can be predicted that the bonds are generally weaker in ethanol and can be more easily broken than in gas phase.

Table 1: Optimized Bond Lengths (Å) of Anthracene molecule
Geometrical

Geometrical parameter	RHF/6-31G		B3LYP/6-31G	
	Gas	Ethanol	Gas	Ethanol
R(1,2)	1.3466	1.3546	1.3739	1.3754
R(1,6)	1.4299	1.4313	1.4288	1.4306
R(1,17)	1.0719	1.0751	1.0854	1.0877
R(2,3)	1.4341	1.4358	1.4329	1.4344
R(2,18)	1.0729	1.0762	1.0864	1.0887
R(3,4)	1.4245	1.4289	1.4491	1.4503
R(3,7)	1.3874	1.3929	1.4036	1.4051
R(4,5)	1.4341	1.4358	1.4329	1.4344
R(4,8)	1.3874	1.3929	1.4036	1.4051
R(5,6)	1.3466	1.3546	1.3739	1.3754
R(5,19)	1.0729	1.0762	1.0864	1.0887
R(6,20)	1.0719	1.0751	1.0854	1.0877
R(7,10)	1.3874	1.3929	1.4036	1.4051
R(7,16)	1.0738	1.0771	1.0873	1.0895
R(8,9)	1.3874	1.3929	1.4036	1.4051
R(8,21)	1.0738	1.0771	1.0873	1.0895
R(9,10)	1.4245	1.4289	1.4491	1.4504
R(9,15)	1.4341	1.4358	1.4329	1.4344
R(10,11)	1.4341	1.4358	1.4329	1.4344
R(11,12)	1.0729	1.0762	1.0864	1.0887
R(11,13)	1.3466	1.3546	1.3739	1.3754
R(13,14)	1.4299	1.4312	1.4288	1.4306
R(13,22)	1.0719	1.0751	1.0854	1.0877
R(14,15)	1.3466	1.3546	1.3739	1.3754
R(14,23)	1.0719	1.0751	1.0854	1.0877
R(15,24)	1.0729	1.0762	1.0864	1.0887

Table 2: Optimized Bond Angles (˚) of Anthracene molecule

Geometrical Parameter	RHF/6-31G		B3LYP/6-31G	
	Gas	Ethanol	Gas	Ethanol
A(2,1,6)	120.5026	120.4908	120.4258	120.4711
A(2,1,17)	120.4399	120.384	120.2436	120.2384
A(6,1,17)	119.0574	119.1251	119.3307	119.2905
A(1,2,3)	120.9085	120.8532	120.9857	120.8877
A(1,2,18)	120.7818	120.7035	120.5779	120.6705
A(3,2,18)	118.3097	118.4433	118.4364	118.4419
A(2,3,4)	118.5889	118.656	118.5886	118.6413
A(2,3,7)	122.1413	122.0701	122.3186	122.1876
A(4,3,7)	119.2698	119.2739	119.0929	119.1712
A(3,4,5)	118.5889	118.6559	118.5885	118.6412
A(3,4,8)	119.2697	119.2743	119.0928	119.1712
A(5,4,8)	122.1413	122.0697	122.3187	122.1877
A(4,5,6)	120.9085	120.8532	120.9856	120.8876
A(4,5,19)	118.3097	118.4426	118.4364	118.4419
A(6,5,19)	120.7818	120.7042	120.578	120.6705
A(1,6,5)	120.5026	120.4909	120.4258	120.4712
A(1,6,20)	119.0577	119.1246	119.3313	119.2911

Table 2: Optimized Bond Angles (˚) of Anthracene molecule ***-continued***

Geometrical Parameter	RHF/6-31G		B3LYP/6-31G	
	Gas	Ethanol	Gas	Ethanol
A(5,6,20)	120.4397	120.3846	120.2428	120.2377
A(3,7,10)	121.4606	121.4519	121.8144	121.6577
A(3,7,16)	119.27	119.2741	119.0931	119.1715
A(10,7,16)	119.2695	119.274	119.0925	119.1708
A(4,8,9)	121.4606	121.4518	121.8144	121.6577
A(4,8,21)	119.2699	119.2744	119.0932	119.1715
A(9,8,21)	119.2695	119.2738	119.0924	119.1708
A(8,9,10)	119.2697	119.2738	119.0928	119.1711
A(8,9,15)	122.1413	122.0698	122.3188	122.1878
A(10,9,15)	118.589	118.6563	118.5884	118.641
A(7,10,9)	119.2697	119.2741	119.0928	119.1711
A(7,10,11)	122.1413	122.0701	122.3186	122.1876
A(9,10,11)	118.589	118.6558	118.5887	118.6413
A(10,11,12)	118.31	118.4435	118.4365	118.442
A(10,11,13)	120.9084	120.8531	120.9856	120.8876
A(12,11,13)	120.7816	120.7034	120.5779	120.6704
A(11,13,14)	120.5026	120.4912	120.4257	120.471
A(11,13,22)	120.4396	120.3836	120.2432	120.238
A(14,13,22)	119.0578	119.1252	119.3311	119.2909
A(13,14,15)	120.5026	120.4903	120.4259	120.4713
A(13,14,23)	119.0578	119.1254	119.331	119.2908
A(15,14,23)	120.4396	120.3842	120.2431	120.2379
A(9,15,14)	120.9084	120.8533	120.9857	120.8877
A(9,15,24)	118.31	118.4431	118.4366	118.4421
A(14,15,24)	120.7816	120.7036	120.5777	120.6702

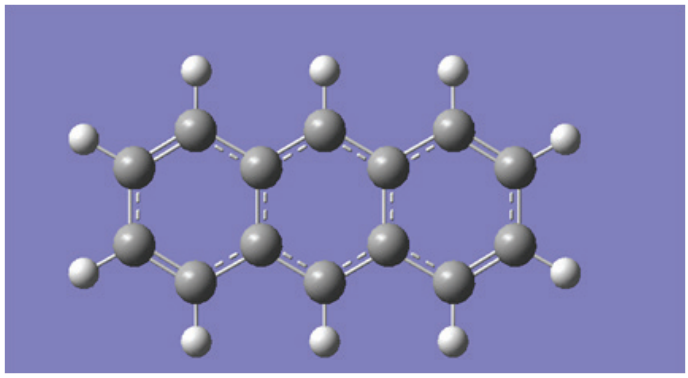

Figure 1: Optimized Structure of Anthracene

For 1-hydroxyanthracene molecule, the optimized bond lengths in gas phase and ethanol are listed in Table 3 while the optimized molecular structure is shown in Figure 2. The changes in bond lengths and bond angles are seen to be similar to the behaviour in Anthracene. An expansion of the molecule on inclusion of electron correlation is indicated in both molecules. In contrast to the case of Anthracene, for 1-Hydroxyanthracene, the replacement of H on the first benzene ring by OH has little effect on the first C-C bond R(1,2). However, the bond length between

the C-O is slightly reduced compared to the C-H in Anthracene. This is due to the fact that O is highly electronegative. The shortest and strongest C-H bond is R(7,15) with a bond length of 1.0712A and 1.0733 Å in gas phase and ethanol at RHF level theory. It is a C-H bond located at the extreme end opposite the O-H group. Thus unlike in the Anthracene molecule where all the C-H bonds are fairly stronger, only R(7,15) is stronger than the rest; though the difference is not much as in R(1,16), R(2,17), R(6,19), R(8,20) etc. It is remarkable to note that the R(24,25) bond has the least bond length of 0.976 Å at RHF and 0.9954 Å at B3LYP level of theory. This is the O-H bond and this is expected due to the electronegativity of oxygen.A(11,24,25), the bond angle between C-O-H is the strongest (Table 4) with an angle of 111.53520 in gas phase at B3LYP level of theory. A(12,11,24), the bond angle between C-C-O is the largest bond angle with a value of 123.27540 in gas phase at RHF level of theory.

Table 3: Optimized Bond Lengths (Å) of 1-hydroxyanthracene molecule

Geometrical Parameter	RHF/6-31G		B3LYP/6-31G	
	Gas	Ethanol	Gas	Ethanol
R(1,2)	1.353	1.3546	1.3744	1.3758
R(1,6)	1.429	1.4309	1.4284	1.4302
R(1,16)	1.0728	1.0751	1.0853	1.0877
R(2,3)	1.4333	1.4349	1.4322	1.4337
R(2,17)	1.0738	1.0763	1.0863	1.0888
R(3,4)	1.4257	1.4269	1.4479	1.4489
R(3,7)	1.3925	1.3938	1.4047	1.4059
R(4,5)	1.4338	1.4353	1.4327	1.4344
R(4,8)	1.3923	1.3934	1.4041	1.4052
R(5,6)	1.3531	1.3547	1.3743	1.3758
R(5,18)	1.0738	1.0762	1.0864	1.0888
R(6,19)	1.073	1.0753	1.0855	1.0877
R(7,10)	1.3881	1.3899	1.4004	1.402
R(7,15)	1.0712	1.0733	1.084	1.0861
R(8,9)	1.3901	1.392	1.4033	1.4052
R(8,20)	1.0744	1.0768	1.087	1.0894
R(9,10)	1.4266	1.4287	1.4477	1.4496
R(9,14)	1.4357	1.4364	1.4335	1.4343
R(10,11)	1.4354	1.4384	1.4361	1.4397
R(11,12)	1.3514	1.3531	1.3749	1.377
R(11,24)	1.3756	1.373	1.3928	1.3871
R(12,13)	1.4286	1.4294	1.4263	1.4269
R(12,21)	1.074	1.0757	1.0867	1.0884
R(13,14)	1.3509	1.3529	1.373	1.3751
R(13,22)	1.0727	1.0751	1.0852	1.0876
R(14,23)	1.0731	1.0755	1.0855	1.0878
R(24,25)	0.9498	0.9671	0.976	0.9954

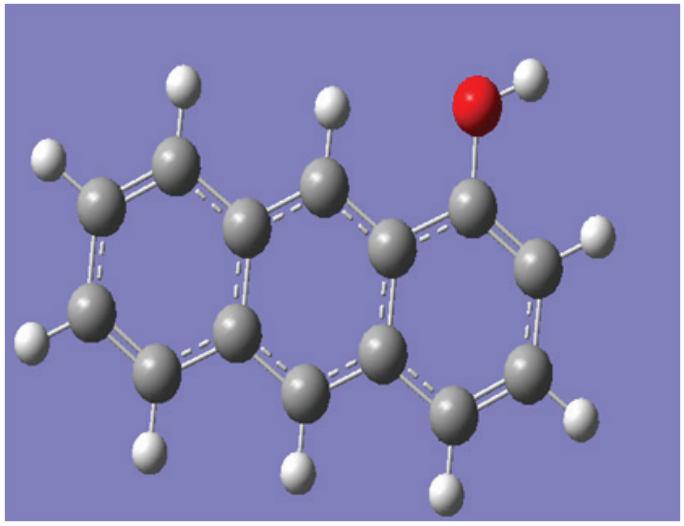

Figure 2: Optimized Structure of 1-Hydroxyanthracene

Generally, there is a slight increase in the bond lengths in moving from RHF/6-31G to B3LYP/6-31G and hence electron correlation increases the size of the molecule. Also, at both levels of theory, it is predicted that the solvent has an effect of expanding the molecule. The bond angles are shown in Table 4 for 1-Hyroxyanthracene.

Table 4: Optimized Bond Angles (°) of 1-hydroxyanthracene molecule

Geometrical Parameter	RHF/6-31G		B3LYP/6-31G	
	Gas	Ethanol	Gas	Ethanol
A(2,1,6)	120.3309	120.4078	120.3754	120.4222
A(2,1,16)	120.4673	120.4433	120.2608	120.2451
A(6,1,16)	119.2018	119.1489	119.3638	119.3327
A(1,2,3)	120.9381	120.8188	120.9605	120.8631
A(1,2,17)	120.6655	120.7416	120.6245	120.6694
A(3,2,17)	118.3964	118.4396	118.415	118.4675
A(2,3,4)	118.7278	118.7769	118.6672	118.7265
A(2,3,7)	121.9342	121.8671	122.097	122.0441
A(4,3,7)	119.338	119.356	119.2358	119.2294
A(3,4,5)	118.5628	118.6385	118.5846	118.6323
A(3,4,8)	119.2596	119.2722	119.0882	119.1086
A(5,4,8)	122.1776	122.0893	122.3272	122.259
A(4,5,6)	120.8873	120.7836	120.9357	120.8449
A(4,5,18)	118.4916	118.4763	118.4857	118.4895
A(6,5,18)	120.6211	120.7401	120.5787	120.6656
A(1,6,5)	120.5531	120.5743	120.4766	120.511
A(1,6,19)	119.1269	119.0811	119.329	119.2845
A(5,6,19)	120.32	120.3446	120.1944	120.2045
A(3,7,10)	121.064	121.1426	121.2818	121.3809
A(3,7,15)	119.9256	119.4074	119.7654	119.319
A(10,7,15)	119.0105	119.45	118.9529	119.3001
A(4,8,9)	121.6237	121.561	121.9413	121.8817
A(4,8,20)	119.2325	119.278	119.1005	119.1424
A(9,8,20)	119.1438	119.161	118.9583	118.9759

A(8,9,10)	118.7871	118.9089	118.5802	118.6881
A(8,9,14)	122.1637	121.947	122.2657	122.1004
A(10,9,14)	119.0491	119.144	119.154	119.2115
A(7,10,9)	119.9277	119.7593	119.8728	119.7113
A(7,10,11)	122.0543	122.186	122.1832	122.2213
A(9,10,11)	118.0181	118.0547	117.944	118.0674
A(10,11,12)	121.5338	121.3448	121.458	121.1943
A(10,11,24)	115.1908	115.4563	115.4156	115.6425
A(12,11,24)	123.2754	123.1988	123.1264	123.1632
A(11,12,13)	119.9423	120.0476	120.0018	120.0838
A(11,12,21)	120.5861	120.2371	120.3778	120.007
A(13,12,21)	119.4716	119.7153	119.6204	119.9092
A(12,13,14)	120.9565	121.0536	120.9042	121.0812
A(12,13,22)	118.5628	118.4782	118.7486	118.6448
A(14,13,22)	120.4807	120.4682	120.3472	120.274
A(9,14,13)	120.5001	120.3553	120.5379	120.3617
A(9,14,23)	118.6428	118.621	118.6997	118.7177
A(13,14,23)	120.857	121.0237	120.7624	120.9205
A(11,24,25)	114.5652	114.6454	111.5352	112.1765

The bond length of Anthracene (Table 1) for C1-C2 was found to be 1.3466Å and 1.3739Å in gas phase at RHF and B3LYP levels of theory respectively. For 1-hydroxyanthracene, C1-C2 bond length in gas phase at B3LYP level of theory is 1.3744Å. These bond lengths for C1-C2 bond differ from that of 2,4,6 trinitrottolune (another derivative of anthracene) for it is 1.411Å at B3LYP/6-31G and 1.406Å at B3LYP/6-311G. Thus Anthracene and 1 Hydroxyanthracene studied in this research work have shorter bond length for C1-C2 bond compared to TNT (Clarkson *et al*., 2003). For C2-C3, C3-C4, and C1-C6 bonds, 2,4,6 trinitrotolune is predicted to have shorter bond lengths than for the molecules studied in this work (Clarkson *et al.*, 2003). This could be due to the heavy F1groups (NO2, CH3) attached to C2, C1 and C6 of 2,4,6 trinitrotolune. Also, a similar trend is observed in the bond angles at B3LYP/6-31G level of theory for the two molecules in gas phase (Clarkson *et al.*, 2003). Clarkson *et al*. (2003) predicted higher values for C5-C6-C1, C3-C4-C5 and C1-C2-C3 bond angles for 2,4,6 trinitrotolune compared to those of the organic compounds studied in this work and vice-versa for C4-C5-C6 and C2-C1-C6. Also, a comparative analysis of the optimized parameters obtained in this study and that of Kukhta *et al.* (2008) revealed a similar trend.

Dipole Moments, Quadrupole Moments and Energies

The dipole moment is the first derivative of the energy with respect to an applied electric field. It is a measure of the asymmetry in the molecular charge distribution and is given as a vector in three dimensions. For Hartree-Fock calculations, this is equivalent to the expectation values of X, Y and Z, which are the quantities reported in the output. The predicted dipole moments (in Debye) at different levels of theory are shown in Table 5. The dipole moment of the molecules gives the strength of the polarity of the molecule. The predicted dipole moment is almost zero at RHF/6-31G level and zero at B3LYP/6-31G level. Thus, the molecule is non polar and the charge distribution is fairly symmetrical.

Table 5: Dipole moments (in Debye) in Gas phase and ethanol.

Molecule	**RHF/6-31G**		**B3LYP/6-31**	
	Gas	**Ethanol**	**Gas**	**Ethanol**
Anthracene	0.0003	0.0003	0.0000	0.0000
1-Hydroxyanthracene	1.2978	1.8605	1.3867	2.1065

Quadrupole moments provide a second order approximation of the total electron distribution, providing at least a crude idea of its shape. One of the components being significantly larger than the others would represent an elongation of the sphere along that axis. If present, the off-axis components represent trans-axial distortion (stretching or compressing of the ellipsoid). The quadrupole moment for the molecule at different levels of theory is shown in Table 6. The molecules are predicted to be slightly elongated along the ZZ axis and this elongation increases in ethanol at the RHF/6-31G and B3LYP/6-31G levels.

Table 6: Quadrupolemoments(in Debye) in Gas phase and ethanol

Molecule	**RHF/6-31G**		**DFT/B3LYP/6-31G**	
	Gas	**Ethanol**	**Gas**	**Ethanol**
	XX YY ZZ	**XX YY ZZ**	**XX YY ZZ**	**XX YY ZZ**
Anthracene	-69.4309 -70.0816 -91.7071	-66.8135 -67.8178 -89.9211	-70.2391-70.9301-86.5803	-66.5629-67.8575-86.9452
1-Hydroxyanthracene	-66.8081 -78.0330 -94.6558	-59.5805 -75.1359 -95.0966	-66.6535 -77.3321 -91.8075	-59.3213 -74.2876 -92.2196

All frequency calculations include thermochemical analysis of the molecular system. By default, this analysis is carried out at 298.15 K and 1 atmosphere of pressure, using the principal isotope of each element type in the molecular system. Predicted total energy, electronic, translational, rotational and vibrational energies in kcal/mol for the molecules both in gas phase and in ethanol are listed on Tables7 and 8.

Table 7: Predicted thermal energies (kcal/mol)

Energy	RHF/6-31G		B3LYP/6-31	
	Gas	Ethanol	Gas	Ethanol
Total Energy	137.058	134.846	129.172	128.283
Electronic Energy	0.000	0.000	0.000	0.000
Translational Energy	0.889	0.889	0.889	0.889
Rotational Energy	0.889	0.889	0.889	0.889
Vibrational Energy	135.281	133.069	127.395	126.506

Table 8: Predicted thermal energies (kcal/mol) for 1-Hydroxyanthracene

Energy	RHF/6-31G		B3LYP/6-31G	
	Gas	Ethanol	Gas	Ethanol
Total Energy	141.165	135.685	132.297	128.469
Electronic Energy	0.000	0.000	0.000	0.000
Translational Energy	0.889	0.889	0.889	0.889
Rotational Energy	0.889	0.889	0.889	0.889
Vibrational Energy	139.388	133.907	130.519	126.691

The translational energy relates to the displacement of molecules in space as a function of the normal thermal motions of matter. Rotational energy is observed as the tumbling motion of a molecule as a result of the absorption of energy within the microwave region. The vibrational energy component is a higher energy term and corresponds to the absorption of energy by a molecule as the component atoms vibrate about the mean center of their chemical bonds. The electronic component is linked to the energy transitions of electrons as they are distributed throughout the molecule, either localized within specific bonds, or delocalized over structures, such as an aromatic ring.

It is seen that the molecules are slightly more stable in gas phase. The difference in total energies from gaseous to ethanol is a bit larger when electron correlation is included. Anthraceneis found to be most stable by approximately 2.20 kcal/mol at RHF/6-31G level and by nearly 0.1 kcal/mol at B3LYP/6-31G in gas phase as compared to ethanol. This shows that the presence of ethanol tends to reduce its stability which may be of importance in its effectiveness in use.

Charge Transfer and Polarizabilities

Within molecular system, atoms can be treated as a quantum mechanical system. On the basis of the topology of the electron density the atomic charges in the molecule can be explained. The electrostatic potential derived charges using the CHelpG scheme of Breneman at different atomic positions in gas phase and in ethanol of Anthracene and 1-Hydroxyanthracene at RHF/6-31G and B3LYP/6-31G levels of theories is given in Tables9 and 10. The Mulliken population analysis partitions the charges among the atoms of the molecule by dividing orbital overlap evenly between two atoms. Whereas the electrostatic potential derived charges assign point charges to fit the computed electrostatic potential at a number of points on or near the Van der Waal surface. Hence, it is appropriate to consider the charges calculated by CHelpG scheme of Breneman instead of Mulliken population analysis.

Table 9: Electrostatic Potential Derived Charges on different atomic positions of Anthracene molecule

S/N	Atom	RHF/6-31G		B3LYP/6-31G	
		Gas	Ethanol	Gas	Ethanol
1	C	-0.099099	-0.086073	-0.070869	-0.087024
2	C	-0.273560	-0.284203	-0.211148	-0.237186
3	C	0.231306	0.242868	0.196931	0.203503
4	C	0.231306	0.233456	0.196931	0.194860
5	C	-0.273561	-0.272865	-0.211150	-0.226797
6	C	-0.099098	-0.099706	-0.070868	-0.099200
7	C	-0.517887	-0.533159	-0.401578	-0.443229
8	C	-0.517887	-0.531535	-0.401578	-0.441837
9	C	0.231304	0.239461	0.196930	0.208845
10	C	0.231304	0.235328	0.196930	0.204879
11	C	-0.273559	-0.274940	-0.211148	-0.235444
12	H	0.156788	0.153876	0.112495	0.133509
13	C	-0.099100	-0.094367	-0.070869	-0.069005
14	C	-0.099100	-0.091341	-0.070868	-0.066114
15	C	-0.273559	-0.279741	-0.211149	-0.240018
16	H	0.240497	0.248847	0.170733	0.199296
17	H	0.123261	0.118999	0.088015	0.091468
18	H	0.156788	0.155712	0.112494	0.129855
19	H	0.156788	0.153936	0.112495	0.128184
20	H	0.123261	0.121830	0.088015	0.093957
21	H	0.240497	0.248328	0.170732	0.198881
22	H	0.123261	0.120323	0.088015	0.112196
23	H	0.123261	0.120020	0.088015	0.111909
24	H	0.156788	0.154947	0.112495	0.134511

Table 10: Electrostatic Potential Derived Charges on different atomic positions of 1- Hydroxyanthracene

S/N	Atom	RHF/6-31G		B3LYP/6-31G	
		Gas	Ethanol	Gas	Ethanol
1	C	-0.097690	-0.132542	-0.099595	-0.111613
2	C	-0.217263	-0.214012	-0.160720	-0.186025
3	C	0.131462	0.112474	0.114131	0.110930
4	C	0.287751	0.284380	0.219171	0.223916
5	C	-0.284951	-0.309088	-0.225100	-0.252941
6	C	-0.054656	-0.064146	-0.051729	-0.062521
7	C	-0.289153	-0.314916	-0.256269	-0.279493
8	C	-0.503317	-0.507640	-0.369869	-0.404971
9	C	0.314298	0.273268	0.186055	0.197469
10	C	-0.032936	-0.010846	0.064237	0.032181
11	C	0.488970	0.399869	0.284261	0.304039
12	C	-0.405742	-0.301968	-0.199257	-0.222094

Table 10: Electrostatic Potential Derived Charges on different atomic positions of 1- Hydroxyanthracene -*continued*

S/N	Atom	RHF/6-31G		B3LYP/6-31G	
		Gas	Ethanol	Gas	Ethanol
13	C	0.013488	-0.044472	-0.062508	-0.073589
14	C	-0.375532	-0.350673	-0.239033	-0.273075
15	H	0.199213	0.199433	0.137688	0.154589
16	H	0.102533	0.129083	0.091041	0.109154
17	H	0.129207	0.142562	0.101308	0.122973
18	H	0.138009	0.161032	0.112010	0.135386
19	H	0.099463	0.121222	0.085159	0.103197
20	H	0.210253	0.238021	0.159853	0.188439
21	H	0.161373	0.195581	0.121013	0.157113
22	H	0.108687	0.117757	0.085133	0.101805
23	H	0.158416	0.165987	0.113962	0.135463
24	O	-0.782639	-0.850615	-0.684062	-0.747682
25	H	0.500757	0.560249	0.473120	0.537348

It is clear from Tables 9 and 10 that the amount of charges on C2, C3, C4, C6, C7, C8, C10, C11, C15, H16 and H21 atoms increases while on C1, C5, C9, H12, C13, C14, H17, H18, H19, H20, H22, H23 and H24 atoms decreases at RHF/6-31G level and at B3LYP/6-31G level decreases in ethanol than that of gas phase charges. It means that former atoms acquire charges from the solvent medium while later atoms loses their charges to the solvent medium due to the effect of the solvent.

Polarizability refers to the way the electrons around an atom redistribute themselves in response to an electrical disturbance. The polarizability tensor components of the molecules in gas phase as well as in ethanol obtained at RHF/6-31+G and B3LYP/6-31+G levels of theory is listed on Tables11 and 12. The polarizability tensor components of Anthracene molecule show a change in goingfrom gas phase to solution at both levels of theory. All the polarizability tensor components (xx, xy, yy, xz, yz and zz) of molecules increase significantly at both levels of theory, but they do not follow any regular pattern. The change in polarizability tensors is more pronounced in ethanol than in the gas phase. This may be due to the fact that the polarity of the solvent (ethanol) and the dipole moments of the molecule are more in ethanol than in the gas phase.

Table 11: Polarizabilities of Anthracene

Orientation	RHF/6-31G		B3LYP/6-31G	
	Gas	Ethanol	Gas	Ethanol
Xx	230.248	346.355	265.371	382.047
Xy	0.000	0.004	0.000	0.004
Yy	136.995	226.380	149.437	227.444
Xz	0.000	0.032	0.000	0.027
Yz	0.001	-0.023	0.000	-0.008
Zz	30.674	47.748	40.085	48.630

Table 12: Polarizabilities of 1-Hydroxyanthracene

Orientation	RHF/6-31G		B3LYP/6-31G	
	Gas	Ethanol	Gas	Ethanol
XX	238.705	353.883	267.757	394.721
XY	-7.090	8.757	7.608	8.648
YY	148.759	236.925	159.427	242.927
XZ	0.002	-4.097	-0.004	-4.096
YZ	0.001	8.334	0.002	6.613
ZZ	40.363	51.119	41.240	52.239

The vibrational spectrum of a molecule is considered to be a unique physical property and is characteristic of the molecule. As such, the infrared (IR) spectrum can be used as a fingerprint for identification by the comparison of the spectrum from an 'unknown' with previously recorded reference spectra. The fundamental requirement for infrared activity, leading to absorption of infrared radiation, is that there must be a net change in dipole moment during the vibration for the molecule or the functional group under study. The vibrational frequency is usually expressed in cm-1 (Lee *et al*., 1988). Another important form of vibrational spectroscopy is Raman spectroscopy, which is complementary to infrared spectroscopy. The selection rules for Raman spectroscopy are different to those for infrared spectroscopy, and in this case a net change in bond polarizability must be observed for a transition to be Raman active (Coates, 2000).

In this work, Gaussian software was used to predict the vibrational spectra of Anthracene molecule in its ground state. These frequency calculations are valid only at stationary points on the potential energy surface, thus our computations were performed on the optimized structures of the molecules. As 6-31G is the smallest basis set that gives satisfactory results for frequency calculations, it was used. Raw frequency calculations computed at the Hartree-Fock level contain known systematic errors due to the neglect of electron correlation, resulting to overestimates of about 10-12%. Therefore, it is usual to scale frequencies predicted at the HF level by an empirical factor of 0.8929. Use of this factor has been demonstrated to produce very good agreement with experiment for a wide range of systems. The values in this study must be expected to deviate even a bit more from experiment because of the choice of a medium-sized basis set (6-31G)- around 15%. For B3LYP/6-31G a scale factor of 0.9613 is used.

Some IR and Raman intense vibrational frequencies and their approximate descriptions for the molecules in gas phase and ethanol at RHF and B3LYP levels with 6-31G basis set are presented in tables 13-16. The frequencies reported are not scaled as is usually done in comparing the similar

calculated frequency with observed frequency (as no experimental results were found for comparison). The B3LYP results show a significant lowering of the magnitudes of the calculated frequencies.

The most intense IR vibrational frequency for Anthracene at RHF level in gas phase is 844.793cm^{-1} (718.636 cm^{-1} in ethanol) corresponding to C-H symmetric stretching of the benzene rings (Table 13), while the most intense Raman vibrational frequency is 1534.75 cm-1 (1549.21 cm^{-1} in solution) corresponding to benzene ring distortions (Table 15). At B3LYP level of theory, the most intense IR vibrational frequency is 3221.85 cm^{-1} in gas phase (3060.08 cm-1 in ethanol) corresponding to C-H anti-symmetric stretching of the ring in plane (Table 14) and the most intense Raman vibrational frequency is 3222.5 cm-1 (3060.44 cm-1 in ethanol) corresponding to C-H symmetric stretching of the benzene rings (Table 16).

Table 13: Some IR Intense Vibrational Frequencies and their Approximate Description for Anthracene Molecule at RHF/6-31G Level of Theory

S/N	Gas	Ethanol	Approximate Description
1	536.672	454.48	C-H symmetric stretching of the rings in plane
2	680.343	582.824	C-C anti-symmetric stretching of the rings
3	844.793	718.636	C-H symmetric stretching of the rings and C-C-H angle bending
4	1058.48	952.081	C-H stretching of the middle ring
5	1819.65	1817.41	C-C anti-symmetric stretching of the rings
6	3367.25	3090.64	C-H anti-symmetric stretching of the rings
7	3381.79	3102.85	C-H symmetric stretching of the rings

Table 14: Some IR Intense Vibrational Frequencies and their Approximate Description for Anthracene Molecule at B3LYP/6-31G Level of Theory

S/N	Gas	Ethanol	Approximate Description
1	760.28	820.3	C-H symmetric stretching of the rings in plane
2	920.096	965.578	C-H symmetric stretching of the rings out of plane
3	3206.92	3048.47	C-H anti-symmetric stretching of the rings in plane
4	3221.85	3060.08	C-H anti-symmetric stretching of the rings in plane

Table 15: Some Raman Intense Vibrational Frequencies and their Approximate Description for Anthracene Molecule at RHF/6-31G Level of Theory

S/N	Gas	Ethanol	Approximate Description
1	430.483	425.675	C-C symmetric stretching of the rings in plane
2	596.25	594.42	C-C anti-symmetric stretching of the rings in plane
3	823.928	824.174	rings breathing
4	894.233	910.791	C-H symmetric stretching of the rings
5	1073.84	1109.59	C-C symmetric stretching of the rings and C-C-H bending
6	1340	1337.08	C-H anti-symmetric stretching of the rings
7	1364.2	1356.32	C-C anti- symmetric stretching of the rings
8	1534.75	1549.21	Ring distortions
9	1730.87	1664.54	C-H anti-symmetric stretching of rings
10	3352.08	3080.47	C-H symmetric stretching of rings
11	3366.85	3090.09	C-H anti-symmetric stretching of rings
12	3382.38	3103.29	C-H symmetric stretching of rings

Table 16: Some Raman Intense Vibrational Frequencies and their Approximate Description for Anthracene Molecule at B3LYP/6-31G Level of Theory

S/N	Gas	Ethanol	Approximate Description
1	773	406.261	C-C symmetric stretching of the rings
2	1047.39	1059.73	C-C anti-symmetric stretching of the rings
3	1451.19	1262.3	Ring distortions
4	1543.41	1332.25	C-C anti-symmetric stretching of the rings
5	1610.48	1499.21	Ring distortions
6	3192.13	3037.5	C-H symmetric stretching of the rings
7	3206.62	3048.18	C-H anti- symmetric stretching of the rings
8	3222.5	3060.44	C-H symmetric stretching of the rings

The various IR and Raman spectra for the molecules at different levels of theory and in different media are shown in figures 3-6 for anthracene and while tables 17-20 and figures 7-10 for 1-hydroxyanthracene respectively.

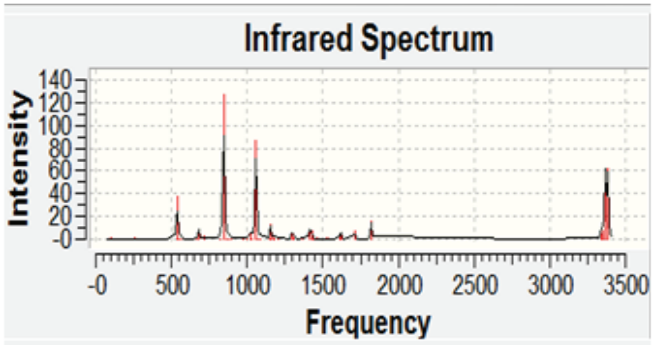

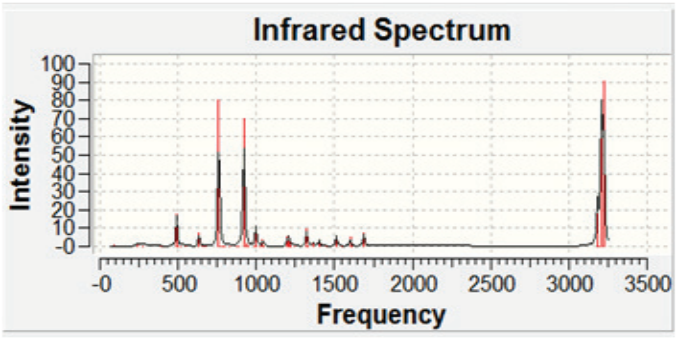

(a) RHF (b) B3LYP

Figure 3: IR Spectrum for Anthracene in Gas Phase

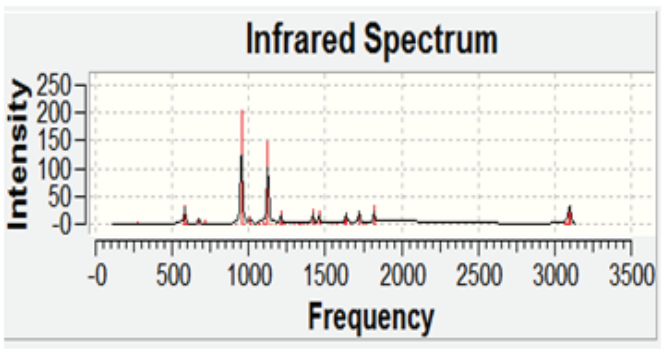

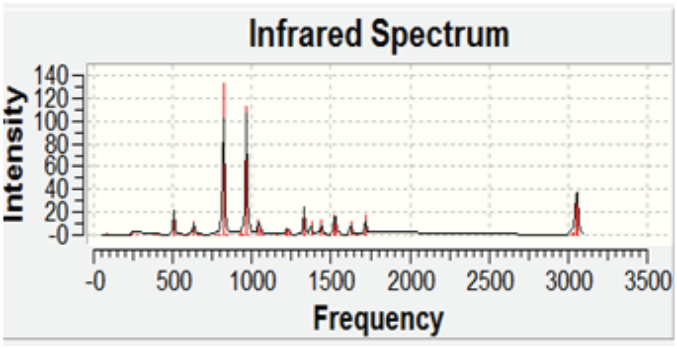

(a) RHF (b) B3LYP

Figure 4: IR Spectrum for Anthracene in Ethanol

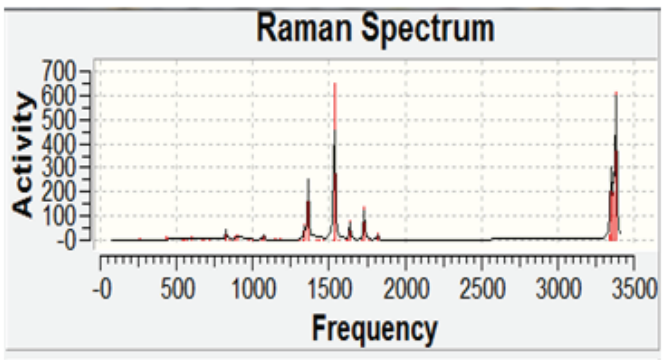

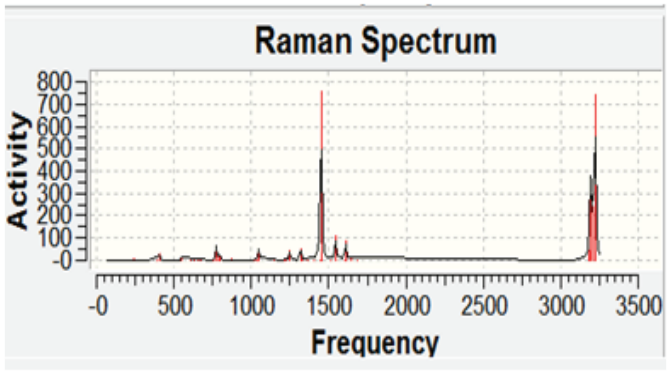

(a) RHF (b) B3LYP

Figure 5: Raman Spectrum for Anthracene in Gas Phase

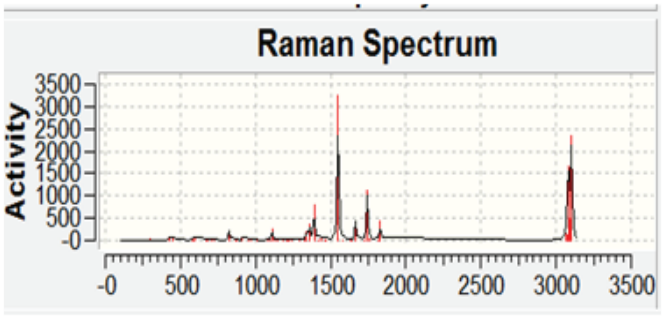

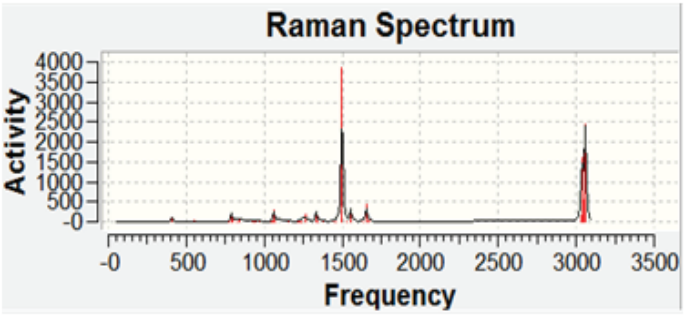

(a) RHF (b) B3LYP

Figure 6: Raman Spectrum for Anthracene in Ethanol

Table 17: Some IR Intense Vibrational Frequencies and their Approximate Description for 1-Hydroxyanthracene Molecule at RHF/6-31G Level of Theory

S/N	Gas	Ethanol	Approximate Description
1	373.799	214.42	O-H stretching in plane
2	841.572	516.284	C-H symmetric stretching of the rings
3	1066.39	960.246	C-H symmetric stretching of the rings
4	1265.13	966.833	C-C anti-symmetric stretching of the rings
5	1416.56	1092.04	C-C anti-symmetric stretching of the rings
6	3385.71	2811.289	C-H symmetric stretching of the rings
7	4046.72	3706.09	O-H stretching in plane

Table 18: Some IR Intense Vibrational Frequencies and their Approximate Description for 1-Hydroxyanthracene Molecule at B3LYP/6-31G Level of Theory

S/N	Gas	Ethanol	Approximate Description
1	391.515	294.388	O-H stretching out of plane
2	756.53	1192.92	C-H symmetric stretching of the rings out of plane
3	1048.06	1269.14	C-C anti-symmetric stretching of the rings
4	1174.49	1326.78	C-C anti-symmetric stretching of the rings
5	1315.13	1345.31	C-C anti-symmetric stretching of the rings
6	1320.41	3709.2	O-H stretching

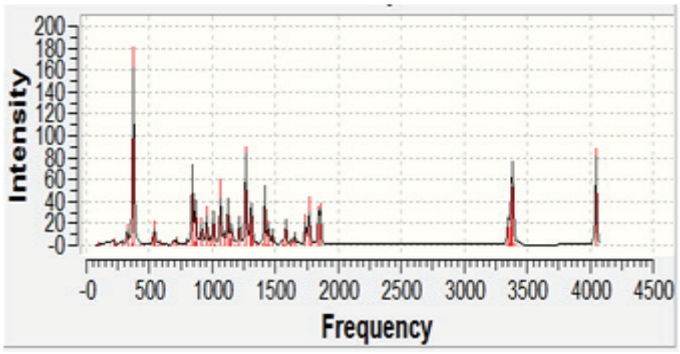

(a) RHF/6-31G

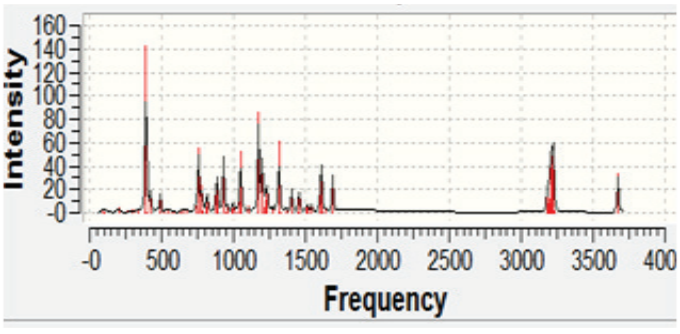

(b) B3LYP/6-31G

Figure 7: IR Spectrum for 1-Hydroxyanthracene in Gas Phase

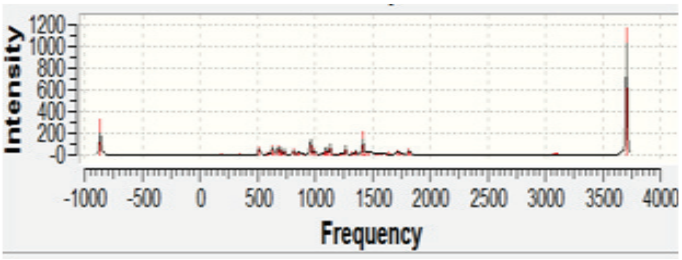

(a) RHF/6-31G

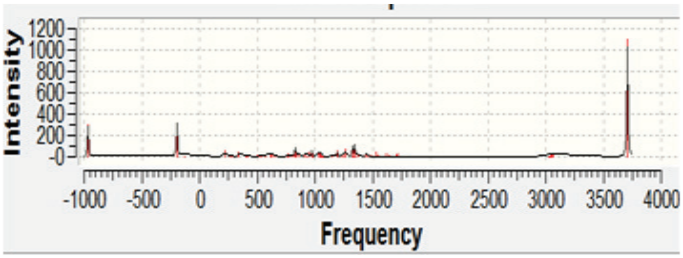

(b) B3LYP/6-31G

Figure 8: IR Spectrum for 1-Hydroxyanthracene in Ethanol

Table 19: Some Raman Intense Vibrational Frequencies and their Approximate Description for 1-Hydroxyanthracene Molecule at RHF/6-31G Level of Theory

S/N	Gas	Ethanol	Approximate Description
1	1352.78	425.044	C-C symmetric stretching of rings
2	1401.31	1095.84	C-C anti-symmetric stretching of rings
3	1563.37	1109.74	C-C anti-symmetric stretching of rings
4	1567.97	1175.08	C-C anti-symmetric stretching of rings
5	1584.39	1217.31	C-C anti-symmetric stretching of rings
6	1655.94	1335.33	C-C anti-symmetric stretching of rings
7	1857.72	1402.4	Ring distortions
8	3350.05	1435.41	C-H symmetric stretching of rings
9	3356.2	1444.36	C-H symmetric stretching of rings
10	3361.95	1577.73	C-H anti-symmetric stretching of rings
11	3372.23	3081.12	C-H anti-symmetric stretching of rings
12	3385.71	3090.54	C-H anti-symmetric stretching of rings
13	3387.49	3098.55	C-H symmetric stretching of rings
14	4046.72	3706.09	O-H stretching in plane

Table 20: Some Raman Intense Vibrational Frequencies and their Approximate Description for 1-Hydroxyanthracene Molecule at B3LYP/6-31G Level of Theory

S/N	Gas	Ethanol	Approximate Description
1	1447.65	403.693	C-C anti-symmetric stretching of rings
2	1454.29	773.704	C-C anti-symmetric stretching of rings
3	1460.4	1058.59	C-C anti-symmetric stretching of rings
4	545.01	1152.48	C-Canti-symmetric stretching of rings
5	1612.99	1192.92	C-C symmetric stretching of rings
6	3184.35	1244.7	C-H symmetric stretching of rings
7	3185.06	1269.14	C-H anti-symmetric stretching of rings
8	3197.74	1326.78	C-H anti-symmetric stretching of rings
9	3206.49	1345.31	C-H anti-symmetric stretching of rings
10	3219.58	1462.41	C-H symmetric stretching of rings
11	3221.65	1508.71	C-H symmetric stretching of rings
12	3229.72	3028.64	C-H symmetric stretching of rings
13	3674.04	3709.2	O-H stretching in plane

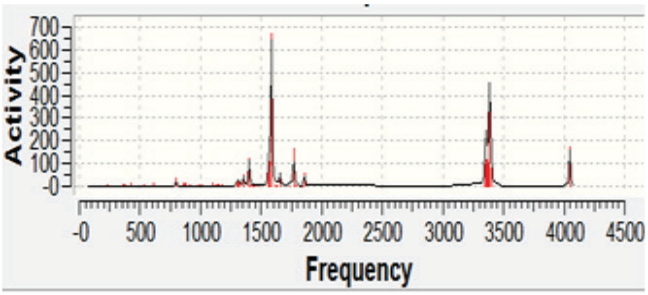

(a) RHF/6-31G

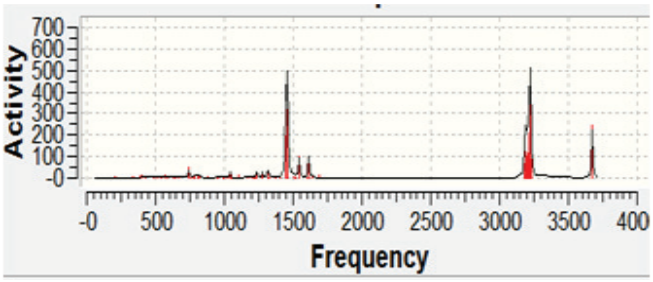

(b) B3LYP/6-31G

Figure 9: Raman Spectrum for 1-Hydroxyanthracene in Gas Phase

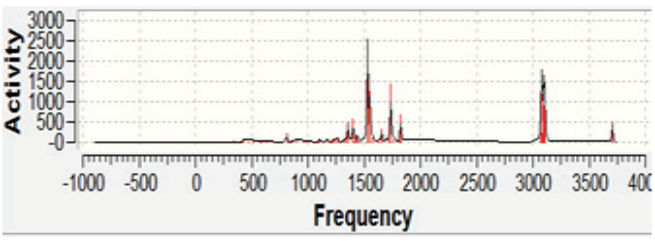

(a) RHF/6-31G

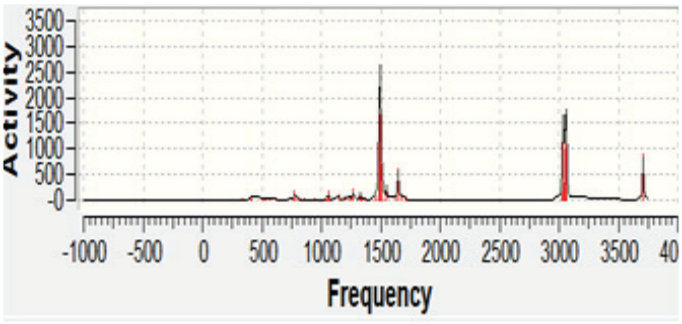

(b) B3LYP/6-31G

Figure 10: Raman Spectrum for 1-Hydroxyanthracene in Ethanol

CONCLUSION

To compliment this research work, the experimental part of this study can be undertaken to ascertain the accuracy of this computational technique. Also, this work can be done using other computational physics software's and results compared with the results in this work. Anthracenecan be studied in other environments to see the effect of these environments on their physical properties. Other solvents that can be considered include hexane, benzene, hydronaphthalenes, Carbon disulfide, Chloroform and other organic solvents.

The practicability of the findings in this work is an encouraging factor. This work provides the fundamental basis for all computational and experimental studies on these molecules vis-à-vis their semi-conducting and opto-electric properties. Our study has exposed the molecular and electronic properties of these molecules for use in the fabrication of organic semiconductor devices.

ACKNOWLEDGEMENT

We are thankful to the Council of Scientific and Industrial Research (CSIR), India for financial support through Emeritus Professor Scheme (Grant No. 21(0582)/03/EMR-II) to Late Prof. A.N. Singh of the Physics Department, Bahamas Hindu University, India which enabled him to purchase the Gaussian Software. We are most grateful to Emeritus Prof. A.N. Singh for donating this software to Physics Department, Gombe State University, Nigeria.

REFERENCES

James, W., (2007). Product engineering: molecular structure and properties. Oxford University Press.

Kimberly, D.M., and Ernest, M., (2011). Coordination Complexes as Catalysts: The Oxidation ofAnthracene by Hydrogen Peroxide in the Presence of VO(acac)2.*Prokopchuk Journal of Chemical Education* 88 (8), 1155-1157

Becke, A.D., (1993). "Density Functional Thermochemistry III.The role of exact exchange", *Journal of Chemical Physics,* 98, 5648

Frisch, M.J., Trucks, G.W., Schlegel, H.B., Scuseria, G.E., Robb,M.A., Cheeseman, J.R., Montgomery, J.A., Vreven Jr.T, Kudin, K.N., Burant, J.C., Millam, M., Iyengar, S.S., Tomasi, J., Barone, V., Mennucci, B., Cossi, M., Scalmani, G., Rega, N., Petersson,G.A., Nakatsuji, H., Hada, M., Ehara, M., Toyota, K., Fukuda, R., Hasegawa, J., Ishida, M.,Nakajima, T., Honda, Y., Kitao, O., Nakai, H., Klene, M., Li, X., Knox, J.E., Hratchian, H.P., Cross, J.B., Adamo, C., Jaramillo, J., Gomperts, R., Stratmann, R.E., Yazyev, O., Austin, A.J., Cammi, R., Pomelli, C., Ochterski, J.W., Ayala, P.Y., Morokuma, K., Voth, G.A., Salvador, P., Dannenberg, J.J., Zakrzewski, V.G., Dapprich, S., Danniels, A.D., Strain, M.C., Farkas, O., Malick, D.K., Rabuck, A.D., Raghavachari, K., Foresman, J.B., Ortiz, J.V., Cui, Q., Baboul, A.G., Clifford, S., Cioslowski, J., Stefanov, B.B., Liu, G., Liashenko, A., Piskorz, P., Komaromi, I., Martin, R.L., Fox, D.J., Keith, T., Al-Laham, M.A., Peng, C.Y., Nanayakkara, A., Challacombe, M., Gill, P.M.W., Johnson, B., Chen, W., Wong, M.W., Gonzalez, C., and Pople J.A(2004. Gaussian 03, Revision C.02, Gaussian, Inc., Wallingford CT, 2004.

Lee, C., Yang, W., and Parr, R.G., (1988), "Development of the Colle-Salvetti correlation-energy formula into a functional of the electron density", *Physical Review* B, 37, 785

Coates, J., (2000). Interpretation of Infrared Spectra, A Practical Approach: *In Encyclopedia of Analytical Chemistry*, R.A. Meyers (Ed.), pp.10815-10837, John Wiley & Sons, Chichester.

Friedrich,D.M., Mathies,R., & Albrecht, A.C. (2004). "Studies of excited electronic states of anthracene and some of its derivatives by photoselection and PPP-SCF calculations", *Jounal of Molecular Spectroscopy*, 74, 90180

Kukhta, A.V., Kukhta, I.N., Kukhta, N.A., Neyra, O.L. & Meza, E. (2011). "DFT study of the electronic structure of anthracene derivatives in their neutral, anion and cation forms" *Journal of Physics* B, 41, 205701

Naoto, A., Masaaki M and Atsushi N. (2007). Comprehensive photoelectron spectroscopic study of anionic clusters of anthracene and its alkyl derivatives: Electronic structures bridging molecules to bulk" *Journal of Chemical Physics*.127, 234305

Skorokhodov, S.S., Krakovjak, M.G., Anufrieva, E.V. & Shelekhov, N.S. (2007). "Investigation of chemical behavior of anthracene derivatives as monomers and reagents in synthesis of macromolecules containing anthracene groups" *Journal of Polymer Science*, 15, 287-295

Liu, J., Jiang, L., & Hu, W. (2009). "The Application of Anthracene and Its Derivatives in Organic Field-Effect Transistors", Progress in Chemistry, 2568-2577

Umar, G., and Chifu E.N. (2012) "Electronic Structure and Properties of the Organic Semiconductor Material Anthracene in Gas phase and ethanol An Initio and DFT Study The African Review of Physics. *The African Review of Physics*, Pp 253-263.